Experimental and numerical study of geothermal rainwater tanks for buildings passive cooling

Lucas Striegel[a,c], Jean-Baptiste Bouvenot[a,c], Edouard Walther[a] and Hossein Nowamooz[b,c]

[a] National Institute of Applied Sciences (INSA); Department of HVAC (Heating, Ventilation, and Air Conditioning) and Energy Engineering, Strasbourg, France
lucas.striegel@insa-strasbourg.fr, CA
jean-baptiste.bouvenot@insa-strasbourg.fr
edouard.warther@insa-strasbourg.fr
[b] National Institute of Applied Sciences (INSA); Department of Civil Engineering, Strasbourg, France
hossein.nowamooz@insa-strasbourg.fr
[c] The Engineering science, computer science and imaging laboratory (ICube Laboratory), Illkirch, France

Abstract:

This communication presents the study of a new hybrid system consisting of a buried rainwater tank thermally activated through a water-to-water heat exchanger. This low-tech solution, little studied in the literature, performs the passive cooling of buildings and reduces domestic water network consumption (for non-potable uses). Firstly, experimental results obtained from two full-scale prototypes are presented. Then, numerical studies are discussed.

Keywords:

Building cooling; Geothermal energy; Measurement-simulation comparison; Rainwater collection; Thermal energy storage.

1. Introduction

With climate change, summer comfort and CO_2-emission reduction are two increasingly relevant topics. In this project, we are trying to develop a low-tech system allowing for the cooling of indoor spaces without using refrigerants or with a reduced energy expense.

The literature review shows a lack of detailed studies of such systems. The exploitation of experimental data of cold and hot water tanks connected to a thermo-active building system was treated by Kaltz [1], where the authors demonstrate that a 11 m^3 cistern could provide about 1000 kWh of cooling energy over a whole year. Simulation studies have been carried out by Upshaw [2] with the study of a non-buried rainwater storage tank. The approach considered the rainwater tank as a means of shifting the electrical peak load of an air conditioning unit. Sodah [3] simulates an open system with an aeration loop enhancing evaporative cooling but calculation is only monthly. While Gan [4], considered a tank with special design heat exchanger as a heat source for a heat pump (active system), which is also different from our approach. Marigo [5], also considered a ground coupled heat pump but the cold source is much closer to the rainwater tank we studied. The ground heat exchanger consists of helical shaped pipe in polyethylene immersed into a concrete-built water tank. The size of the tank and pipe are almost the same as our prototypes. To the best of our knowledge, the modelling of variable free-surface water storage and the related mass and heat transfers involved appears to be poorly documented.

To set up the model, the physical equations from both usual domestic water tanks and atmospheric reservoirs were combined, taking into account heat transfer between air and water. We hence aim here at establishing and validating an equation-based physical model, using the data of two full-scale prototypes in operation since July 2021.

In further works, the model will be coupled with a state-of-the-art building energy simulation tool in order to estimate the relevance of the system regarding summer comfort.

This work is organised as follows: first the principle of the system is explained, then the experimental setup and results are described and eventually a first version of numerical model and simulation is presented.

2. Main concept of the Rainergies system

The basis of the solution described consists in a new or existing buried rainwater tank, initially used for rainwater collection as non-potable domestic water and the relief of sewage networks. In France, the water resources management legislation locally enforces the water management at parcel level which could democratize the use of such rainwater tank. A helicoidal water-to-water heat exchanger (HX) is placed in the tank in order to take advantage of the heat storage capacity of water as a by-product. Thanks to an air-to-water heat exchanger connected to the ventilation supply duct, the tank delivers cooling energy to the building during summer [6].

In summary, the "Rainergies" system consist in following elements:

- A water tank for rain collection,
- A water/water coil heat exchanger immersed in the rainwater tank,
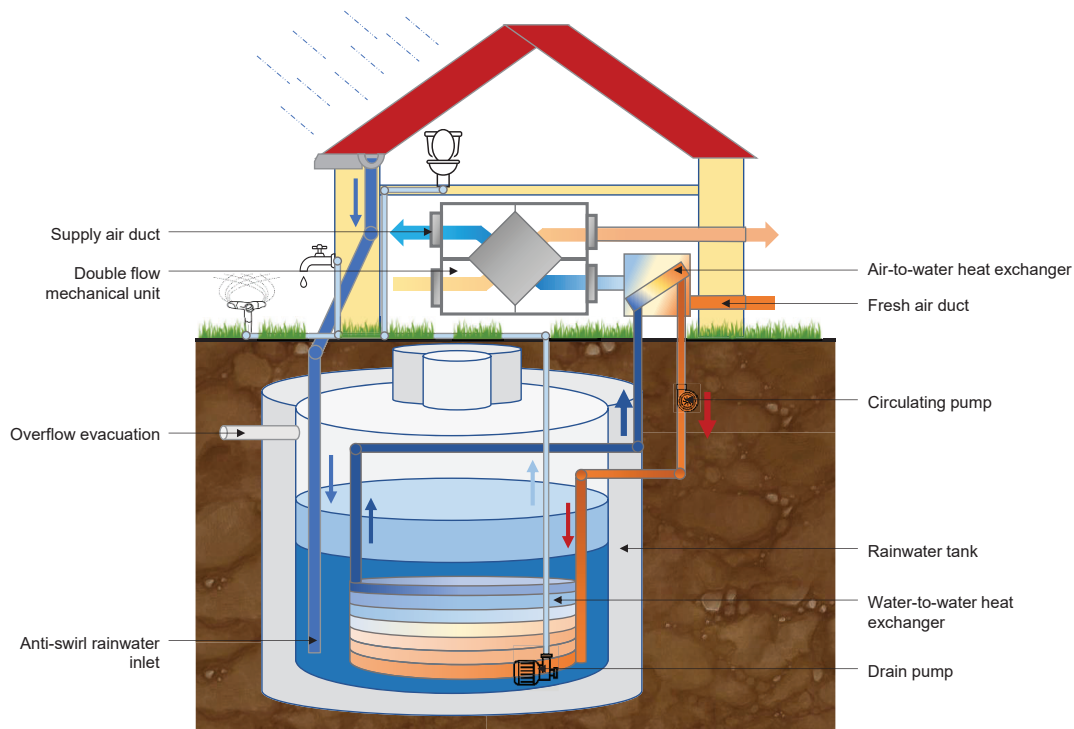- A water/air heat exchanger placed after the supply air duct and connected to the immersed coil.

Figure. 1. Schematic diagram of the Rainergies principle (not at scale).

3. Experimental Study

3.1. Experimental set-up

Three Rainergies prototypes are installed in different locations in Alsace, France, in a semi-continental climate [7]. For the sake of conciseness, this article focuses on one prototype, located in Haguenau.

It consists of a 11 m^3 tank made of precast concrete with a coppered hundred-meter-long coiled heat exchanger. The surrounding ground is dry sand. A 1 kW cooling coil, placed before the double flow air handling unit, allows the heat transfer from the water loop to the supply air ventilation of a 150 m² family house which dates from the 1930's but has been retrofitted lately to match current standards of the French building energy code.

Another prototype, also installed in a residential house, is very similar. The third system is located under a small office building with a larger tank of 25 m^3 and two immersed coils.

These prototypes will be the topic of a future communication, allowing to compare results with different setups (*e.g.* the position of the coil in the double flow mechanical ventilation) and ground properties (sandstone and groundwater flow).

2704

3.2. Measurements

Presently, the Haguenau prototype is monitored with more than 25 sensors connected to dataloggers, with a minimum timestep of 10 min. The devices were installed in the summer 2021 and consolidated data is available since early 2022. The main measured data are:

- Water temperature stratification thanks to 5 fixed dataloggers evenly distributed over the height of the tank (0 m, 0.5 m, 1 m, 1.5 m, 2 m).
- Water level through total pressure of the bottom of the tank.
- Air temperature and humidity inside the tank.
- Temperatures at the air-to-water heat exchanger limits (both air and water).
- Meteorological data including rainfall, global solar radiation, air temperature and humidity.
- Temperature inside the buildings (at air vent and in the room)

3.3. Experimental Results

The results observed in winter operation mode and summer operation are encouraging.

During summer operation, as observed on Figure 2, the system can decrease the supply temperature of the ventilation by up to 13 °C, keeping indoor temperatures of the monitored houses under 27°C during the 2022 summer heatwave. The cooling energy between the 14th of May to 1st of September reached 455 kWh (considering an average ventilation flow rate). The average cooling power is 365 W but peaks of 1 kW were observed. Measurements show little variation of the air-to-water heat exchanger efficiency between [0.64 ; 0.88] with an average of 0.82 ± 0.16 which is consistent with the design value.
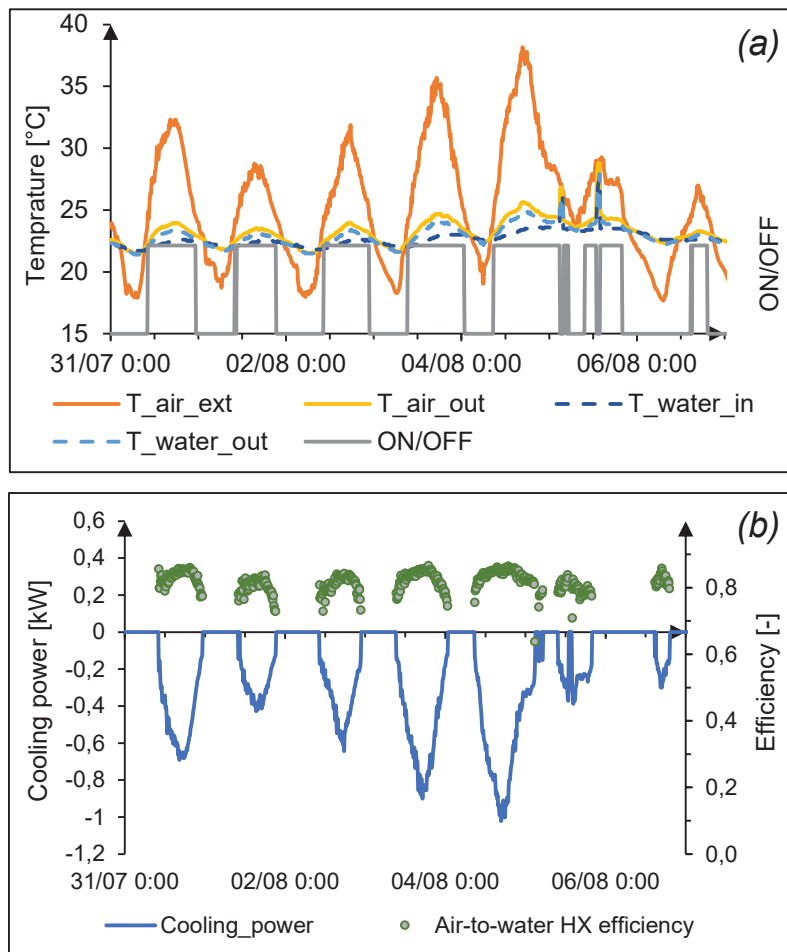
Figure. 2. Air-to-water heat exchanger, summer operation (a) and its cooling power produced and efficiency (b) (2022 – Week 31 – Haguenau).

In winter, it is also possible to use the energy in the tank for preheating before it passes through the double flow ventilation. This preheating is necessary to protect the ventilation elements from freezing in case negative outdoor temperatures. It is usually provided by an electrical heater. On the Haguenau prototype, this phenomenon was observed during 120 h over the winter period 2021-2022 (November 1st to March 15th), corresponding to ~ 39 kWh saved. The power supplied reaches 500W (average of 230W) and the air temperature was maintained above 0 °C despite outdoor dry bulb temperatures of - 6 °C (see Figure 3).

Thus, the system also allows for energy savings in winter (though in moderate quantities). Noticeably, winter operation allows to cool down the reservoir and its surrounding ground, which is beneficial for summer operation, as it participates to a seasonal energy storage.
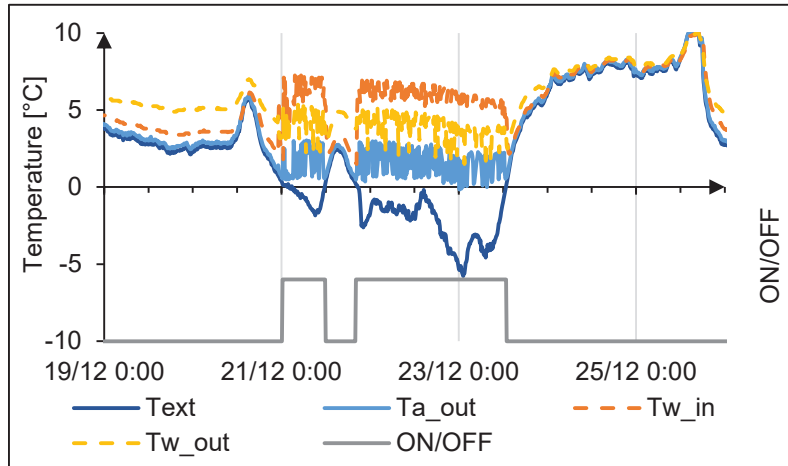
Figure. 3. Air-to-water heat exchanger, winter operation (2021 – Week 51 – Haguenau).

One of the difficulties of this project is to well assess the input parameters and their influence on the system behaviour. The experimental observation phase of the project can help to highlight and understand these events. For example, during rainfall the water temperature inside the tank is influenced by the quantity of rain but also its temperature (see Figure 3 – "T_Xm" meaning that the temperature sensor is at X m starting from the bottom of the tank) : during rainy events, for similar quantities water the temperature in the tank may drop significantly differently (up to 3 K). As this phenomenon is not observed after each rainfall, the hypothesis can be made that the temperature of the rain arriving in the tank is in cause. This parameter is difficult to evaluate, depending on pressure, air temperature but also probably of the roof surface temperature (harvesting surface) however recording the temperature inside the tank rainwater filter will allow in the future to validate the rain temperature model chosen.
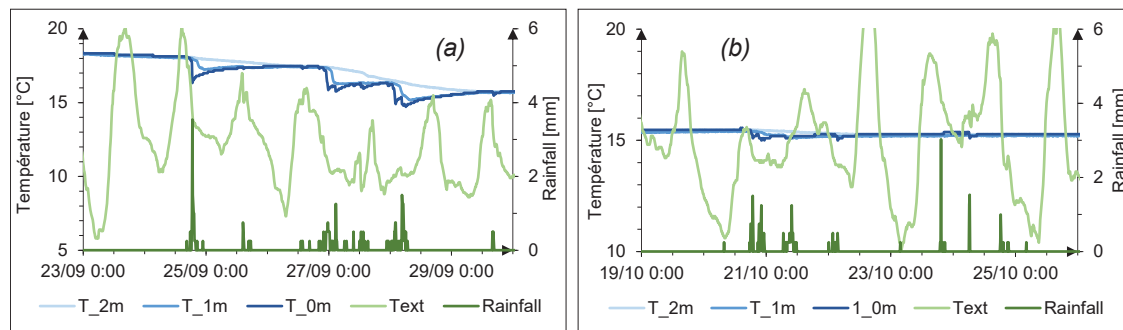
Figure. 4. Rainwater tank during rainy event with influence on the water temperature (a) and without influence (b) (2022 - Week 39 - Haguenau).
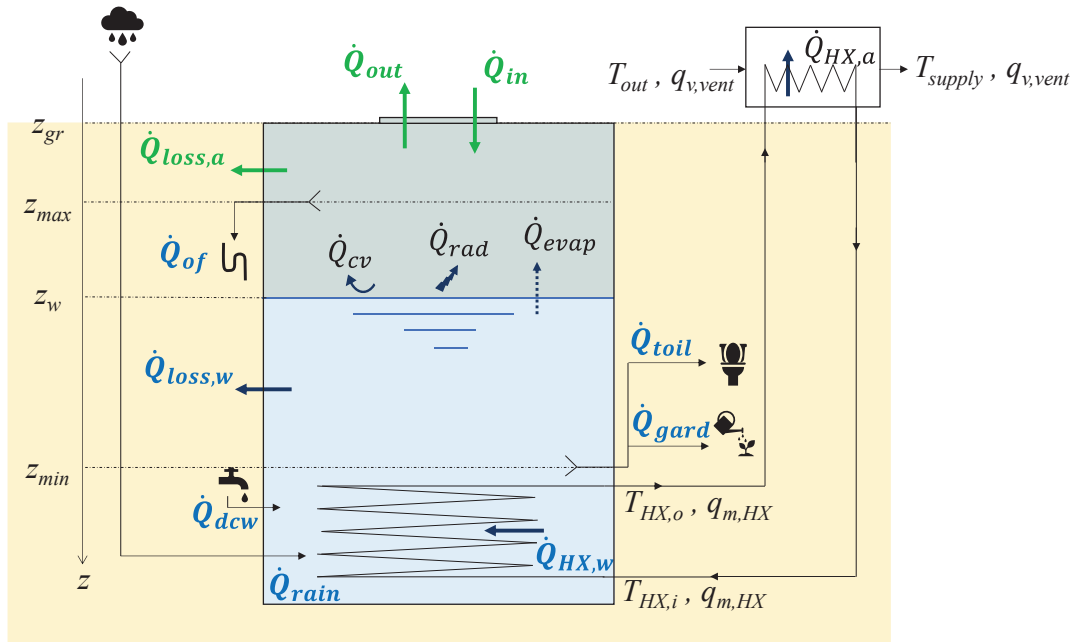
4. Numerical Modelling

Figure. 5. System thermal balance.

4.1. Tank model

In first approach the tank is modelled with two temperature nodes, the ambient air temperature T_a (Eq. (2)) and the water temperature T_w (Eq. (1)), computed through the following thermal balances (a graphical representation of notations is given in Figure 5).

$$\rho_w c_{p_w} \frac{dV_w T_w}{dt} = -\dot{Q}_{loss,w} - \dot{Q}_{cv} - \dot{Q}_{rad} - \dot{Q}_{evap} + \dot{Q}_{HX,w} + \dot{Q}_{rain} + \dot{Q}_{dcw} + \dot{Q}_{toil} + \dot{Q}_{gard} + \dot{Q}_{of} \quad (1)$$

$$\rho_a c_{p_a} \frac{dV_a T_a}{dt} = -\dot{Q}_{loss,a} + \dot{Q}_{cv} - \dot{Q}_{out} + \dot{Q}_{in} \quad (2)$$

The different heat flows $\dot{Q}_X$ are detailed below, starting with the water node thermal balance.

- $\dot{Q}_{loss,w} = U_{w,gr} S_w \left(\overline{T_{w,gr}} - T_w \right)$ represents the convective and conductive losses from the water through the wall with $U_{w,gr}$ the heat transfer coefficient, taking into account the convection and conduction resistance, and $\overline{T_{w,gr}}$ the weighted mean temperature of the ground adjacent to water,.

- $\dot{Q}_{cv} = h_{c,a-w} S_{w-a} (T_a - T_w)$ is the convective flux between the water and the air, with $h_{c,a-w}$ the convection coefficient.

- $\dot{Q}_{rad} = h_{r,w-w} S_{w-a} (\overline{T_{wall}} - T_w)$ stand for the radiative exchange between the surface water and the wall above it, with $h_{r,w-w}$ the linearized radiative coefficient and $\overline{T_{wall}}$ the weighted mean temperature of the wall.

- $\dot{Q}_{evap} = q_{m,evap} L_v$ is the latent loss due to water evaporation, with L_v the vaporization latent heat and $q_{m,evap}$ the evaporation mass flow rate computed thanks to Hen's correlation [8].

- $\dot{Q}_{HX,w} = q_{m,HX} c_{p,gw} (T_{HX,o} - T_{HX,i})$ represents the heat flux extracted from the water-to-water heat exchanger.

- $\dot{Q}_{rain} = q_{m,rain} c_{p,w} T_{rain}$ is the heat flux due to precipitation and is treated as an advection flux. The same approach is used for the district cold water intakes, toilet flushing, gardening, or overflowing withdrawals represented by $\dot{Q}_{dcw}, \dot{Q}_{toil}, \dot{Q}_{gard}, \dot{Q}_{of}$ respectively.

The air node thermal balance is presented below.

- $\dot{Q}_{loss,a} = U_{a,gr}S_a(\overline{T_{a,gr}} - T_a)$ expresses also the convective and conductive losses through the wall but on the air side (similarly $U_{a,gr}$ stand for the heat transfer coefficient and $\overline{T_{a,gr}}$ the weighted mean temperature of the ground in contact with the air.

- $\dot{Q}_{out} = (q_{m,out} + q_{m,leak})T_a$ is an advection flux considering the air volume changes and the air leakage from the tank to the outside. $\dot{Q}_{in}$ is its counterpart but from the outside to the tank.

The inlet and outlet temperatures of the coil are computed through both equations of the air-to-water and water-to-water heat exchanger. As mentioned in the experimental results section, the air-to-water heat exchanger efficiency does not vary much, hence it is assumed constant which is also consistent with the forced convection that takes place in the exchanger. For the first simulations, the same hypothesis has been made for the water-to-water heat exchanger efficiency. The supply air temperature is determined by the equilibrium of the heat flow at the air-water heat exchanger.

4.2. Ground model

The ground is assumed to be homogeneous with constant properties not depending on the soil moisture. As the heat transfer is symmetrical according to the z axis, the 2D heat transfer equation in cylindrical coordinates was used:

$$\rho c_p \frac{\partial T}{\partial t} = \lambda \left(\frac{\partial^2 T}{\partial z^2} + \frac{\partial^2 T}{\partial r^2} + \frac{1}{r}\frac{\partial T}{\partial r} \right) \tag{3}$$

The numerical model for the heat equation is a discrete finite volume formulation of Equation (3). Depending on the volume location, thermal properties are adapted. A source term is added on the superficial node to consider the solar radiation. In this first model, the spatial discretisation is constant with 50 cm mesh, but it is intended that following models integrate a variable space discretisation with local refinements around the tank. The variation of ground moisture content is not modelled in this first model.

4.3. Solving Procedure

In order to solve simultaneously for the air, water and ground temperatures, the semi-implicit Crank-Nicolson numerical method was used as described by Walther [9]. It has the advantage of unconditional stability and is of second order in space and time.

5. Model validation

5.1. Simulation hypothesis

Input parameters, such as weather data or geometrical parameters, are extracted from measured prototype data. Glycol water mass flow and air ventilation flow are considered constant respectively at 0.14 kg.s^{-1} according to the design value and 240 m^3.h^{-1} according to one-off measurement values. Convection coefficients were assessed for steady state and kept constant throughout the simulation.

Marigo [5] using a previous study of Kusuda and Achenbach [10] explains that ground temperatures without thermal perturbations (*e.g.* geothermal probe or buried tank) depend on ground properties and outside air conditions (average annual air temperature and annual air temperature amplitude) :

$$T_{ground}(z,t) = T_m - A_T e^{-z\sqrt{\frac{\pi}{\alpha \tau_{year}}}} \cos\left(\frac{2\pi}{\tau_{year}}\left(t - t_0 - \frac{z}{2}\sqrt{\frac{\tau_{year}}{\alpha\pi}} \right) \right) \tag{4}$$

T_m is the annual average air temperature (°C), A_T is the annual amplitude of monthly average air temperature [°C], α is the ground thermal diffusivity (m^2.s^{-1}), τ_{year} is the annual periode (s) and t_0 is the date of the minimum surface temperature (s). Figure 6. shows the ground temperature variation as function of depth from the surface during the year, which is relatively stable at a 10 m depth. The ground temperature is therefore assumed constant at a depth of 10 meters below ground level (lower boundary condition). The soil temperature for $0 < z < 10$ m is initialised according to this model.
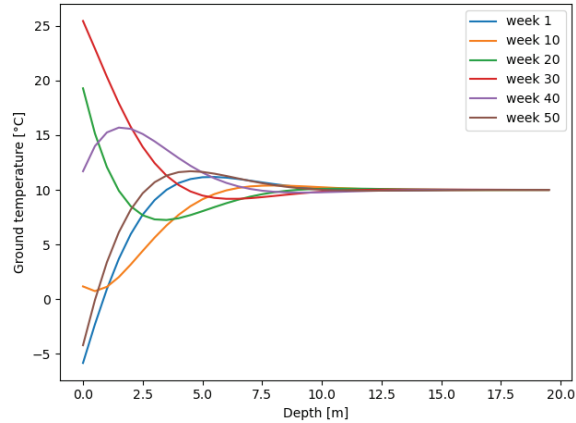
Figure. 6. Calculated ground temperature against depth for several week in Haguenau

The outdoor weather data are used as boundary condition for ground surface (temperature, wind and solar flux).

The input parameters are summarized below.

**Table 1.** Input parameters of the conducted simulation.

Parameter	value
Simulation parameters	
Timestep	600 s
Spatial step through z axis	0.5 m
Spatial step through radial axis	0.5m
Geometrical dimensions	
Tank diameter	2.5 m
Tank height	3 m
Roof surface	180 m²
Ground domain depth	10 m
Ground domain radius	10 m
Material properties	
Ground thermal conductivity	0.7 W.m^{-1}.K^{-1}
Ground heat capacity	850 J.kg^{-1}.K^{-1}
Ground density	1600 kg.m^{-3}
Heat transfer coefficients	
Water-to-water HX efficiency	0.7
Air-to-water HX efficiency	0.8
Water to tank wall convection coefficient	20 W.m^{-2}.K^{-1}
Air to tank wall convection coefficient	7 W.m^{-2}.K^{-1}
Air to water surface convection coefficient	6 W.m^{-2}.K^{-1}

5.2. Numerical results

The prototype setup was simulated over the summer period (from the 14/05/22 to the 31/08/22), using the boundary conditions described in previous section.

The simulation results obtained are presented on Figure 6, depicting the simulated versus measured water tank temperature (above) and the supply air temperature (below). This first model exhibits a correct behaviour in terms of dynamics of the phenomenon, although the magnitude of variations can possibly be fine-tuned.

Considering the simplifications made, the numerical results are very encouraging: the dynamics of water and air temperatures are respected and the simulated water-to-water heat exchanger inlet and outlet temperature and air supply temperature globally match the experimental data.
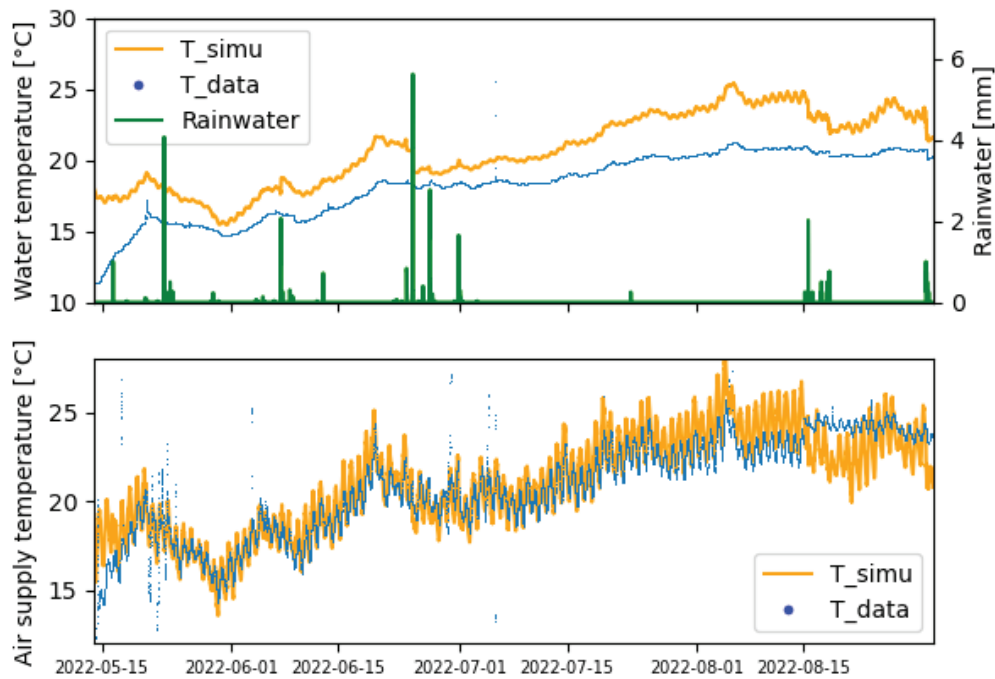
Figure. 7. Experimental and numerical data

Table 2. Root mean square error (RMSE) between numerical and experimental results

| Analysed output	Root Mean Square Error (°C)
Air tank temperature	1.62
Water tank temperature	2.66
Inlet HX temperature	1.09
Outlet HX temperature	1.19
Supply temperature	1.22

In terms of RMSE, the preliminary simulation results obtained are as follow: the highest error is made on the tank temperature prediction (2.77 K) and errors of the order of 1.09 to 1.62 K are made on other temperatures.

In order to reduce the discrepancy between model and measurement, a sensitivity analysis of the model to its input parameters was undertaken.

5.3. Sensitivity analysis

In order to identify the influential parameters of the model, with the intention to obtain a better fit between model and measurements, a preliminary sensitivity analysis was conducted. We used Morris' [11] "one-at-a-time" sensitivity analysis method, taken up by Campolongo [12], which provides a ranking of parameters with an acceptable computational expense, given the involved simulation time (*id est* approximately 2 hours computation for 1 month simulated). The principle of Morris' method, nowadays widely used in the building simulation community, consists in computing the average elementary effect of the variation of one parameter at a time, usually for a dozen of repetitions. This was performed using the state-of-the-art SAlib python library.
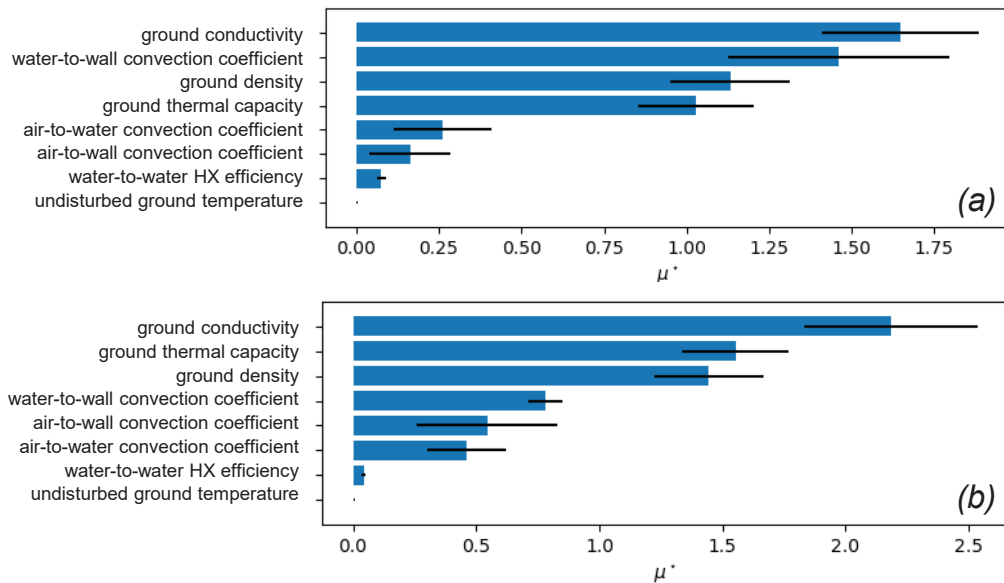
Figure. 8. Elementary effects of Morris's sensitivity analysis on the water tank temperature (a) and on the air tank temperature (b)

The investigation focusses on ground properties, thermal convection coefficients and the efficiency of the water-to-water heat exchanger.

The results obtained on the water tank temperature and air tank temperature are presented on Figure 7. Similar studies were also conducted on the inlet and outlet heat exchanger temperature and on the supply air temperature. The conductivity of ground, the thermal capacity of the ground and the density of ground are the three first influent parameters. The reservoir wall convective transfer coefficient of water is also influent on the water tank temperature.

The results show that following parameters are particularly influent on the outputs:

- All ground properties are significant on the water temperature output. Therefore, assessing those coefficients will be crucial for future work.

- The convection coefficient between wall and water, which calls for the numerical implementation of a temperature dependent correlation.

As a sequel, a parametric fit optimisation on the most influent parameters will be undertaken, with the aim of obtaining a better prediction of the measured temperatures.

6. Discussion

On the experimental side, the primary results exhibit good result with outside air temperature reduction of more than 10 K and cooling power reaching 1 kW. Noticeably, this system does not aim at replacing air conditioning, but it can reduce its use, especially in high-performance buildings. During winter, the prototype can pre-heat the air to protect the installation from frosting, saving the use of an electrical heater.

It is foreseen to conduct data acquisition within shorter timestep to try to better understand short-timed event such as rainfall and its impact on the rainwater tank temperature.

Regarding numerical aspects, ensuing the sensitivity analysis, a parameter fitting procedure will be lead in order to minimize the discrepancy between the model and measurements. Moreover, the models need improvement which have already been planned. The rainwater tank needs to integrate the water stratification and a better evaluation of air leakage which can strongly influence both air and water temperature. Thermal convection coefficients and water-to-water heat exchanger efficiency need also a finer calculation, *e.g.* depending on the air or water temperature instead of constant values. The time calculation will also be enhanced by changing the solving method and switching to a sparse linear algebra library. It will allow shorter time calculations and thus offer more options in terms of sensitivity analysis but also optimization.

7. Conclusion and perspectives

Coupling the model with a building energy simulation tool will allow in future works to optimize the controls and test the solution in different conditions (climate, …). It is also planned to explore the use of a dew point cooler that can provide extra cooling power by water evaporation into exhaust or supply air.

Moreover, with the rise of drought frequency, the applications of rainwater collection may widen, for example with the use of rainwater for laundry. This raises several new questions about the quality of the water stored in the tank. The water temperature increase may lead to microbiologic development, which can make the water unsuitable for certain uses (such as supply for washing machine). It is also possible for a biological film to develop on the heat exchanger leading to fouling and deterioration of its performance. This problem is not very common and deserves some investigation.

The applicability of such systems in real configurations, the performance prediction and the determination of design guidelines is obviously one of the objectives of the research conducted here, be it for commercial buildings or housing applications.

Acknowledgments

Nomenclature

c_p	heat capacity, $J.kg^{-1}.K^{-1}$
D	diameter, m
h_c	convection coefficient, $W.m^{-2}.K^{-1}$
HX	heat exchanger
$\dot{Q}$	heat flux, W
q_m	mass flow, $kg.s^{-1}$
q_v	volume-flow, $m^3.h^{-1}$
RMSE	Root Mean Square Error
T	temperature, K
z	altitude, m

Greek symbols

α	thermal diffusivity, $m^2.s^{-1}$
λ	thermal conductivity, $W.m^{-1}.K^{-1}$
ρ	density, $kg.m^{-3}$
τ	oscillation period

Subscripts and superscripts

a	air
cv	convection
dcw	district cold water
$evap$	evaporation
$gard$	garden
gr	ground
HX,a	air to water heat exchanger
HX,w	water to water heat exchanger
HX,i	heat exchanger inlet
HX, o	heat exchanger outlet
in	to tank inside air
$loss,a$	wall in contact with the air
$loss,w$	wall in contact with the water
of	overflow
out	to outside
$toil$	toilet
rad	radiative

vent   ventilation

w   water

References

[1] D. E. Kalz, J. Wienold, M. Fischer, and D. Cali, Novel heating and cooling concept employing rainwater cisterns and thermo-active building systems for a residential building, Applied Energy, vol. 87, no 2, p. 650-660, Feb 2010.

[2] C. R. Upshaw, J. D. Rhodes, and M. E. Webber, Modeling electric load and water consumption impacts from an integrated thermal energy and rainwater storage system for residential buildings in Texas, Applied Energy, vol. 186, p. 492-508, Jan 2017.

[3] M. S. Sodha, R. L. Sawhney, and D. Buddhi, Use of evaporatively cooled underground water storage for convective cooling of buildings: An analytical study, Energy Conversion and Management, vol. 35, no 8, p. 683-688, Aug 1994.

[4] G. Gan, S. B. Riffat, and C. S. A. Chong, A novel rainwater–ground source heat pump – Measurement and simulation, Applied Thermal Engineering, vol. 27, no 2-3, p. 430-441, Feb 2007.

[5] Marco Marigo, Enrico Prataviera, Sara Bordignon, Michele Bottarelli, and Angelo Zarrella, Analysis of the thermal performance of a water storage cell with helical shaped pipe for ground source heat pumps, presented at Building Simulation 2021, Bruges, Belgium, Sept 2021, p. 8.

[6] J.-B. Bouvenot, Performance simulation of a hybrid geothermal rain water tank coupled to a building mechanical ventilation system, presented at Building Simulation 2021, Bruges, Belgium, Sept 2021.

[7] M.-O. SIU, Rainergy : Conception de prototypes de récupérateurs d'eau de pluie géothermiques, INSA Strasbourg, Strasbourg, Projet de fin d'études, 2021.

[8] H. Hens, Indoor climate and building envelope performance in indoor swimming pools, Energy efficiency and new approaches, Istanbul Technical University: 543-52, 2009

[9] E. Walther, Building Physics - Applications in Python. Paris: DIY Spring, 2021.

[10] T. Kusada and P.R. Achenbach, Earth temperature and thermal diffusivity at selected stations in the United States, ASHRAE Trans 71(1), p. 61-74, 1965.

[11] M. D. Morris, Factorial Sampling Plans for Preliminary Computational Experiments, Technometrics, vol. 33, no 2, p. 161-174, May 1991.

[12] F. Campolongo, J. Cariboni, and A. Saltelli, An effective screening design for sensitivity analysis of large models, Environmental Modelling & Software, vol. 22, no 10, p. 1509-1518, Oct 2007.